Formation and Entrapment of Noble Metal Clusters in Silica Aerogel Monoliths by γ-Radiolysis

Jared F. Hund,[†] Massimo F. Bertino,*[,†] Guohui Zhang,[‡] Chariklia Sotiriou-Leventis,*[,‡] Nicholas Leventis,*[,‡] Akira T. Tokuhiro,[§] and John Farmer[||]

Department of Physics, University of Missouri−Rolla, Rolla, Missouri 65409, Department of Chemistry, University of Missouri−Rolla, Rolla, Missouri 65409, Department of Nuclear Engineering, University of Missouri−Rolla, Rolla, Missouri 65409, MURR, University of Missouri-Columbia, Columbia, Missouri 65211

Received: June 21, 2002; In Final Form: August 21, 2002

Noble metal clusters (Ag, Au) were formed in a silica aerogel matrix by γ-irradiation of hydrogel precursors loaded with aqueous solutions containing Ag^+ or $[AuCl_4]^-$ ions. Hydrogels exposed to γ-rays assumed the color expected for colloidal suspensions of Ag (respectively Au) clusters. The hydrogels were subsequently washed and supercritically dried, without any evident change in color, indicating that the metal clusters were not removed during drying. Typical γ-ray doses were between 2 and 3.5 kGy, and achieved complete reduction of hydrogels containing ion concentrations in the $10^{-4}-10^{-3}$ M range. Reduction of solutions with higher metal ion concentrations was achieved by multiple irradiations. In the case of Ag^+ reduction, we noticed that the radiolytic yield G was higher than that of the reducing radicals equal to $G = 6 \times 10^{-7}$ mol/L of reducing species per joule of absorbed energy. For example, a total dose of 3.5 kGy has led to a reduction of 5.7×10^{-2} M in a hydrogel with $[Ag^+] = 0.1$ M. The high radiolytic yield has been attributed to radiation-induced oxide surface catalysis, or to autocatalysis, but the precise mechanism has not been determined. Metal clusters in the aerogel monoliths were characterized with optical absorption, transmission electron microscopy, X-ray diffraction, scanning electron microscopy, and X-ray photoelectron spectroscopy. These techniques have shown that the clusters have a crystalline fcc structure. Au clusters consist of pure Au, while surface oxidation of Ag clusters was observed with XPS.

Introduction

In situ formation and entrapment of metal clusters in aerogels is desirable for application in catalysis,[1,2] sensors,[3] waste disposal,[4,5] and electromagnetic shielding. Metal clusters have been formed in aerogels by adding to a hydrogel a precursor, generally an organometallic compound, that does not leach out during the wash cycles required prior to the final supercritical drying procedure. High-temperature treatment of the dry aerogel leads to reduction and deposition of the metal particles.[1,2] Alternatively, colloidal metal particles have been added directly into the sol during gelation, and remain trapped all the way to the final aerogel.[6,7]

Another efficient method of reducing metal ions to form homo- and heteronuclear clusters of transition metals is via γ-radiolysis of aqueous solutions.[8−15] That process is initiated by formation of solvated electrons, e_{aq}^- (eq 1),

$$H_2O \xrightarrow{\gamma\text{-radiation}} e_{aq}^-, H_3O^+, H^\bullet, OH^\bullet, H_2O_2 \qquad (1)$$

which reduce metal ions M^{m+} to metal atoms (eqs 2, 3):

$$e_{aq}^- + M^{m+} \rightarrow M^{(m-1)+} \qquad (2)$$

$$e_{aq}^- + M^+ \rightarrow M_0 \qquad (3)$$

Metal atoms eventually form aggregates, M_n (eq 4):

$$nM_0 \rightarrow M_2 \rightarrow \ldots M_n \qquad (4)$$

In this paper, we describe the formation of nanoscopic metal clusters induced by γ-irradiation of a hydrogel in which the gelation solvent (CH_3OH) has been exchanged by an aqueous solution containing ions of the desirable metal (Ag and Au). Typical workup of the resulting metal-cluster-embedded hydrogels leads to aerogel−metal cluster nanocomposites. The materials were characterized with optical absorption, transmission and scanning electron microscopy, X-ray photoelectron spectroscopy, and X-ray diffraction. Our results show that the noble metal clusters have a crystalline fcc structure with lattice parameters comparable to those of the bulk materials, and a cluster size distribution between 10 and 200 nm. Au clusters are free of contamination, while surface oxidation of the Ag clusters has been observed.

The main advantage of our technique is its versatility. For example, it is known that radiolysis allows formation of nonequilibrium alloy clusters such as Au cores surrounded by a Ag shell.[9] Such structures are not accessible by simple impregnation methods, where cluster formation is achieved through high-temperature treatment, which leads to equilibrium

* Corresponding authors. E-mail: massimo@umr.edu, cslevent@umr.edu, leventis@umr.edu.
[†] Department of Physics, University of Missouri−Rolla.
[‡] Department of Chemistry, University of Missouri−Rolla.
[§] Department of Nuclear Engineering, University of Missouri.
[||] MURR, University of Missouri-Columbia.

10.1021/jp026358u CCC: $25.00
Published on Web 12/18/2002

structures. Furthermore, radiolysis can be used to synthesize clusters out of a wide array of noble and transition metals, such as Ni, Co, and Pb.[10]

Experimental Section

Materials. Silica aerogel composites were prepared by a modification of previously published procedures in which the contents of vial A (4.514 mL of tetramethoxysilane; 3.839 mL of methanol) and of vial B (4.514 mL of methanol; 1.514 mL of water, and 20 μL of concentrated NH_4OH) are mixed thoroughly to form a sol that gels at room temperature in 10−15 min.[3] The gels were left to age at room temperature for ~2 days. Aged gels were removed from their molds and soaked in water, four times, for 12 h each time. The water-washed gels were washed again for four times, 12 h each time, with an aqueous solution of the desired metal ion. Such solutions were prepared using $AgNO_3$, $HAuCl_4$, and 2-propanol. The metal ion concentrations in the bathing solutions was varied from 10^{-4} M to 1 M. 2-Propanol was added with a typical concentration of 0.2 M to scavenge the $H^\bullet$ and $OH^\bullet$ radicals generated during irradiation (eq 1). Because of their photosensitivity, all samples were stored in the dark. After the fourth washing, the solution surrounding the gels was decanted. The vials were closed tightly to avoid loss of solvent (water) by evaporation, and they were placed in close proximity to the core of the campus nuclear reactor (see irradiation procedure). At the end of the irradiation period, the gels were visibly darker (depending on the concentration and chemical identity of the metal ions). The vials were filled with water and the gels were allowed to equilibrate for 12 h. That process was repeated another four times. Subsequently, the metal-impregnated gels were washed with acetone (four times, 12 h each time). The pore-filling acetone was replaced in an autoclave with liquid CO_2, and finally the gels were dried supercritically.[3]

Irradiation Procedure. The samples were irradiated with γ-radiation from the fission products of the campus nuclear reactor (Source A).[16] The irradiation procedure was as follows. The reactor was operated at 180 kW for a period of 1−2 h. To prevent neutron bombardment and activation, the samples were placed in front of the core 1 h after reactor shutdown. Due to the decay of the fission products, dose rates decreased from an initial value of about 1 kGy h^{-1} to about 0.4 kGy h^{-1} at the end of the irradiation period (several hours). The mean energy of the γ-rays is 1.12 MeV half an hour after reactor shutdown, and decreases to 0.98 MeV at the end of the irradiation period. Typical total doses were up to about 3.5 kGy per run, as measured by thermoluminescent dosimeters (TLD) placed in vials adjacent to those containing the samples. Typically, γ-rays yield 6 reducing species (solvated electrons and 2-propanol radicals) per 100 eV of deposited energy, or, equivalently, 6×10^{-7} M per joule of absorbed energy. Thus, a dose of 1 kGy can reduce about 5.7×10^{-4} M of Ag^+. Our typical doses of 3−3.5 kGy achieved 100% metal ion reduction for Ag^+ samples with a concentration below about 2×10^{-3} M. Reduction of Au^{III} requires three times as many electrons as Ag^+, so the maximum Au concentration that could be reduced per run was about 7×10^{-4} M. These values of the radiolytic yield apply strictly only to dilute aqueous solutions, but can probably be extended to most of our samples, since they have a low silica content. Given a bulk density of our native silica aerogels of about 0.12 ± 0.01 g/cm^3, and a skeletal density of bulk silica of about 2.4 g/cm^3, we estimate that skeletal silica occupies 5% v/v of the aerogel monoliths, leaving 95% v/v of empty space. Thus, silica accounts for only about 5% of the volume of the irradiated hydrogels, or 12% of their weight. Radiolytic yield of aqueous solutions containing less than 20% w/w of silica is less than 10% higher than the yield of pure water.[17,18] This correction is within the error of the TLD readings (±10%), which are thus reported uncorrected.

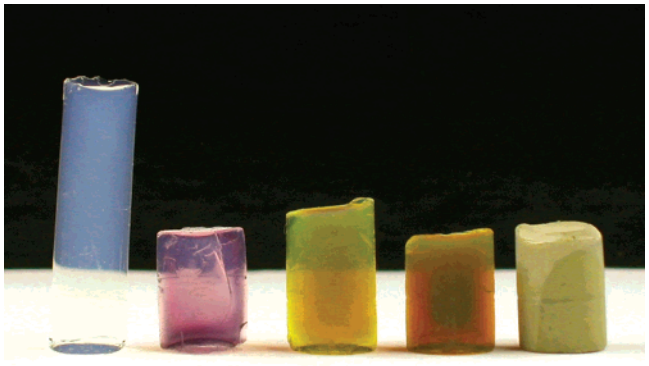

Figure 1. Photographs of native and metal-loaded silica aerogel monoliths. From left: silica aerogel; $[Au^{III}] = 10^{-4}$ M; $[Ag^+] = 10^{-4}$ M; $[Ag^+] = 10^{-3}$ M; $[Ag^+] = 0.18$ M. Note the different colors, and the opacity of the 0.18 M $[Ag^+]$ aerogel.

Alternatively, a few samples were irradiated with a ^{60}Co source located at University of Missouri—Columbia (Source B), which generates dose rates of about 18 kGy h^{-1}. Source B was employed to prepare aerogel/cluster composites with high metal concentrations whose reduction would otherwise require an excessively long time with Source A.

Aerogel Characterization. Photographs of the aerogel composites were obtained with a Nikon Coolpix 5000 digital camera under ambient laboratory illuminations. Optical absorption was measured with a Cary 500 spectrophotometer. X-ray photoelectron spectroscopy (XPS) was carried out on a Kratos Axis 165 scanning spectrometer equipped with a 225-W Mg monochromatized X-ray source, producing photons with an energy of 1253.6 eV. Survey data was taken at a pass energy of 80 eV. Surveys were taken over areas as large as 120 μm^2 to ensure that noble metal clusters were distributed uniformly throughout the aerogel volume. X-ray diffraction (XRD) was measured with a Scintag PadX diffractometer, equipped with a Cu Kα source. Scanning electron microscopy (SEM) was performed with a Hitachi S-4700 microscope equipped with a field emission electron gun. Transmission electron microscopy (TEM) was carried out with a Philips EM430T microscope, operated at 300 keV. TEM measurements were taken by crushing the aerogels and depositing some powder on a carbon-coated copper grid. Selected area electron diffraction (SAED) was used to characterize cluster structure and determine lattice parameters. Local chemical composition was determined with energy-dispersive X-ray chemical analysis (EDS). BET surface area measurements were carried out with a Quantachrome Autosorb-1 instrument.

Results and Discussion

γ-Irradiation deeply affects the color of metal-loaded hydrogel monoliths. Hydrogels with low metal concentrations (10^{-4} to 10^{-2} M) irradiated with γ-rays (mostly from Source A) assume the typical color of colloidal suspensions of metal clusters, i.e., pink for Au, brownish for Ag. Hydrogels with higher metal concentration ($\geq 10^{-1}$ M) become opaque. The color of the monoliths does not change after supercritical drying, indicating that the metal clusters are firmly embedded in the silica matrix. Figure 1 shows images of several aerogels containing varying

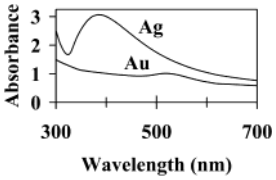

Figure 2. Optical absorption of Ag- and Au-doped aerogel composites obtained by irradiation with Source A of hydrogels made out of solutions having concentrations $[Ag^+] = 10^{-4}$ M, and $[Au^{III}] = 10^{-4}$ M, respectively.

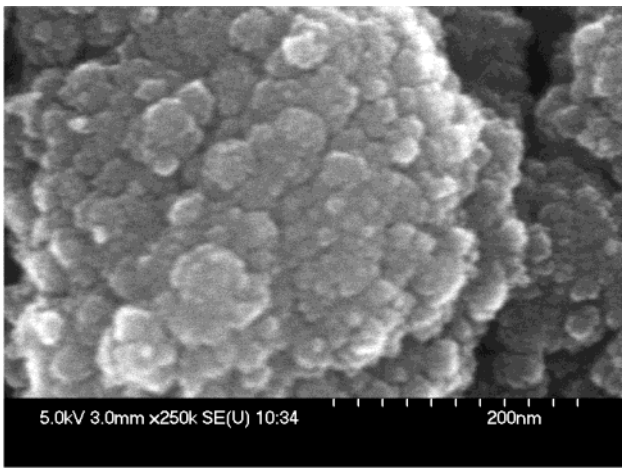

Figure 3. SEM micrograph of a Ag-aerogel composite originating from a $[Ag^+] = 10^{-2}$ M bathing solution.

TABLE 1: Densities, Surface Areas, and Mean Pore Diameter of Aerogel Composites Loaded with Different Metals and Metal Ion Concentrations

reduced amount (M)	metal	density (g/cm^3)	surface area (m^2/g)	mean pore diameter (nm)	monolith color	metal loading (% w/w)
10^{-4}	Ag	0.108	734 ± 100	8.24 ± 1	brown	0.01
10^{-3}	Ag	0.108			dark brown	0.1
0.18	Ag	0.128	776 ± 100	6.80 ± 1	opaque	15
1	Ag	0.1347			opaque	75
10^{-4}	Au	0.116			pink	0.02
10^{-4}	Au	0.133	879 ± 100	9.62 ± 1	pink	0.015
10^{-3}	Au	0.156			pink	0.126

concentrations of Ag and Au, and, for comparison, of a native silica monolith.

Figure 2 shows typical optical absorption spectra of Au- and Ag-loaded silica aerogel monoliths. The absorption maximum of the Ag-doped aerogels is at 385 ± 2 nm, while the maximum of the Au-doped aerogels is at 518 ± 2 nm. These values lie within the range of values previously reported for the plasmon absorption of Au and Ag metal clusters,[19,20] and confirm the presence and chemical identity of metal clusters in both irradiated hydrogel and aerogel composites.

The structure of the aerogels was not fundamentally affected by the synthesis procedure, or by the presence of the clusters. Figure 3 shows SEM micrographs of an Ag−aerogel composite doped with a 10^{-2} M Ag^+ solution. The bead structure of silica is evident, and similar to that reported for native silica aerogels.[3] Table 1 reports the measured densities, surface areas, and pore diameters of aerogels for various metal loadings. We note that the density values are larger, but still comparable with those of pure silica aerogels (0.003−0.010 g/cm^3).[7] Surface areas and mean pore sizes are in the 700−900 m^2/g and 7−10 nm range, respectively, close to the values reported for native silica aerogels (700−1000 m^2/g and 8−14 nm, respectively).[3,7,20,22]

Synthesis of aerogel composite materials with relatively high metal concentrations ($\geq 10^{-2}$ M) was also attempted. This was first attained with Source A by irradiating samples multiple times. Samples could be irradiated several times without any noticeable change in color, or formation of precipitates between consecutive runs. Multiple irradiation allowed us, for example, to generate monoliths loaded with a Au^{III} concentration of 10^{-3} M. For the Ag-loaded monoliths, we noticed that samples coming from bathing solutions with $[Ag^+] \sim 10^{-2}$ M were considerably darker than samples from solutions with a concentration of 2×10^{-3} M, even after one run. At first, this was surprising, since the maximum Ag^+ concentration that can be reduced in one run is about 2×10^{-3} M, i.e., the monoliths should have had the same color. To clarify this discrepancy, and to determine the actual amount of metal ions reduced during each run, the aqueous washings following irradiation were combined, NaCl was added to precipitate AgCl, and the amount of precipitate was determined gravimetrically. It was found that a dose of 3.5 kGy reduced 5.7×10^{-2} M of Ag^+, and a dose of 10−11 kGy reduced ~0.18 M of Ag^+, independent of the initial Ag^+ concentration in the hydrogel monolith. The yield of about 1.6×10^{-2} M $[Ag^+]$/kGy is about 30 times higher than the theoretical value for dilute aqueous solutions of 5.7×10^{-4} M $[Ag^+]$/kGy. There are several possible reasons for this high radiolytic yield. For example, it could be related to the presence of silica in the hydrogels, since the radiolytic yield of silica−water solutions is higher than the yield of pure water.[17] However, the silica content of our hydrogels was fairly low, about 12% w/w, and the additional radiolytic yield should be of the order of 10%.[17] We are more inclined to attribute the higher radiolytic yield to catalytic processes. For example, radiation-induced chemical reactions can take place at oxide surfaces,[18] and there is also evidence for the ability of 2-propanol to reduce Ag^+ ions in basic medium through an autocatalytic process.[23] The radiolytic yield of Ag showed a complicated dependence on metal concentration, dose rate, and 2-propanol concentration. For example, the yield was only about 4 times higher than the theoretical value for hydrogels doped with a solution with $[Ag^+] = 6$ M, and [2-propanol] = 4 M, exposed with Source B to a dose of 400 kGy at a dose rate of 18 kGy/h.

TEM images of Ag- and Au-loaded silica aerogels are reported in Figure 4. Figure 4a shows several metal particles embedded in a large silica flake. SAED and EDS showed that the metal clusters are free of contamination, and have fcc structure. Size distributions of metal particles were determined by measuring a large number of particles from several different images. These are reported in Figure 4b−d for Ag^+ concentrations in the bathing solutions varying from 10^{-4} M to 0.18 M. The mean particle size increases with increasing $[Ag^+]$, from about 45 nm at 10^{-4} M to about 65 nm at 5×10^{-2} M, to about 170 nm at 0.18 M. This particle size dependence on concentration is an indication that cluster growth dominates on cluster nucleation, i.e., nuclei form in the initial stages of reduction, and keep growing, without any (or few) new nuclei being added. Figure 4e shows the size distribution of a sample originating from a solution with $[Au^{III}] = 10^{-4}$ M. Particles are somewhat smaller than those in the Ag sample coming from the same bath concentration, and the mean Au particle size is about 30 nm.

Synthesis of aerogels with very high metal loadings would require irradiation for several weeks with the low-intensity Source A, thus we made a few attempts using the more intense Source B. Figure 5 shows TEM images of a hydrogel coming from a bathing solution with $[Ag^+] = 6$ M, exposed to a total

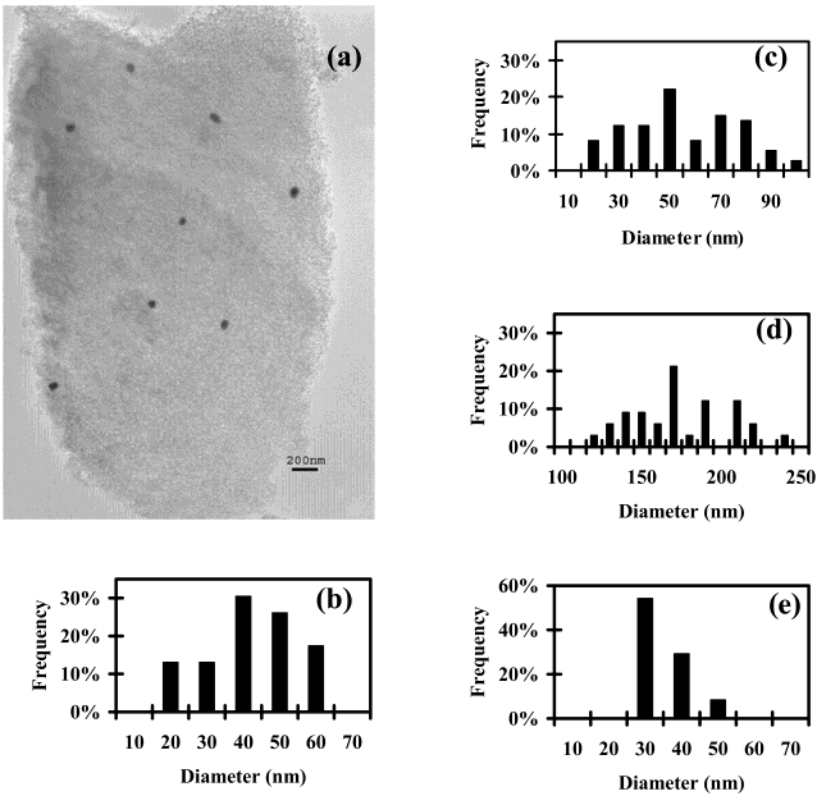

Figure 4. (a) Bright-field TEM micrograph of a 5.7×10^{-2} M [Ag^+] aerogel. (b) Size distribution histogram of a 10^{-4} M [Ag^+] aerogel (23 particles measured). (c) Size distribution of a 5.7×10^{-2} M [Ag^+] aerogel (73 particles measured). (d) Size distribution histogram of a 0.18 M [Ag^+] aerogel (25 particles measured). (e) Size distribution histogram of a 10^{-4} M [Au^{III}] aerogel (24 total particles). Samples irradiated with Source A.

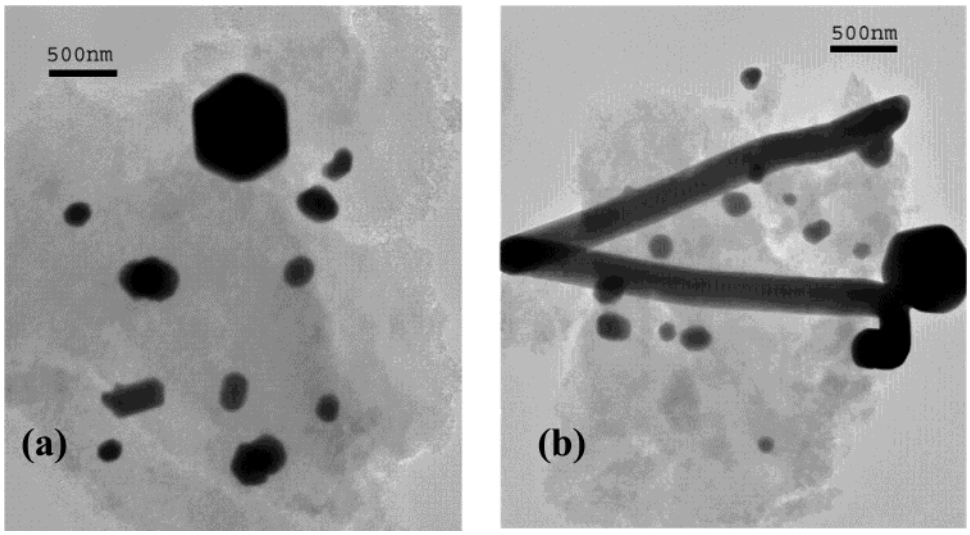

Figure 5. Bright-field TEM micrographs of Ag particles obtained after irradiation with Source B of a 6 M [Ag^+] hydrogel. (a) Example of low aspect ratio particles. (b) Example of high aspect ratio particles. Total dose was 400 kGy, and the dose rate was 18 kGy h^{-1}.

dose of 400 kGy. Thermogravimetric analysis showed that the amount of metal retained inside the aerogel was about 1 M. TEM shows a comparatively small number of large particles with a diameter of several hundred nanometers. In some cases, the particles have rodlike shapes, as shown in Figure 5b.

As for the structure of the metal clusters, analysis of XRD and SAED results was consistent with fcc structures for both Ag and Au. XRD results are reported in Figure 6 for a 5.7×10^{-2} M [Ag^+] bathing solution aerogel, and show (100) and (200) reflections of a fcc structure with the lattice parameter of bulk Ag. From the width of the peaks, an average size of 25 nm was calculated, in fair agreement with the data of Figure 4c.

Figure 7 reports XPS spectra of a 0.5 M [Ag^+] aerogel. The electron binding energy of the 3d states is shifted toward lower energies compared to the bulk. Such shifts are characteristic of oxidized Ag species.[24] Ag oxidation is understandable, considering that the supporting matrix is an oxide and that the synthesis mechanism proceeds, in basic medium, via an Ag_2O intermediate.[23] Oxide states are probably superficial, since XRD analysis is consistent with a fcc structure with the lattice parameter of bulk Ag.

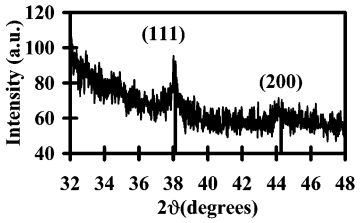

Figure 6. XRD of a Ag−aerogel composite coming from a bathing solution with $[Ag^+] = 5.7 \times 10^{-2}$ M. The vertical lines mark expected peaks for reflection from (111) and (200) planes of bulk Ag.

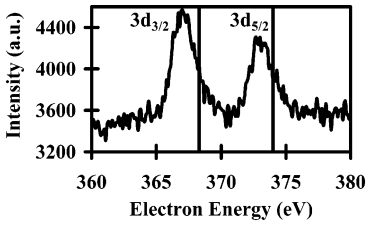

Figure 7. XPS of a 5.7×10^{-2} M $[Ag^+]$ aerogel sample. The vertical lines indicate the position of peaks for bulk Ag. The measured binding energies are lower than the bulk value and are characteristic of oxidized Ag.

In conclusion, we have described a method for the synthesis of metal cluster/aerogel composites. The new materials retain the characteristics of aerogels with a metal content of up to 75% w/w. Work is under way to demonstrate the ability of our method to synthesize clusters of nonnoble metals, like Ni, and cluster alloys. These are well-known characteristics of the radiolysis technique, and can be employed to tailor the physical and chemical properties of aerogel/metal composites.

Acknowledgment. We thank Mr. W. Bonzer for his assistance with gamma irradiation. We also thank Dr. S. Miller for his assistance with the TEM analysis, and Dr. T. Schuman for helpful discussions. Support from the Department of Energy through the Reactor Instrumentation and Reactor Sharing Grant Program is gratefully acknowledged. This work was supported in part by the Petroleum Research Fund (Grant No. 35154-AC5, to N.L. and C.S.-L.).

References and Notes

(1) Piccaluga, G.; Corrias, A.; Ennas, G.; Musinu, A. *Sol−Gel Preparation and Characterization of Metal-Silica and Metal Oxide-Silica Nanocomposites*; Materials Science Foundations, Trans Tech Publications: 2000.

(2) Suh, D. J.; Park, T.-J.; Lee, S.-H.; Kim, K.-L. *J. Non-Cryst. Solids* **2001**, *285*, 309.

(3) Leventis, N.; Elder, I. A.; Rolison, D. R.; Anderson, M. L.; Merzbacher, C. I. *Chem. Mater.* **1999**, *11*, 2837.

(4) Woignier, T.; Reynes, J.; Phalippou, J.; Dussossoy, J. L.; Jacquet-Francillon, N. *J. Non-Cryst. Solids* **1998**, *225*, 153.

(5) Reynes, J.; Woignier, T.; Phalippou, J. *J. Non-Cryst. Solids* **2001**, *285*, 323.

(6) Tai, Y.; Watanabe, M.; Kaneko, K.; Tanemura, S.; Miki, T.; Murakami, J.; Tajiri, K. *Adv. Mater.* **2001**, *13*, 1611.

(7) Anderson, M. L.; Morris, C. A.; Stroud, R. M.; Merzbacher, C.; Rolison, D. R. *Langmuir* **1999**, *15*, 674−681.

(8) Belloni, J.; Mostafavi, M.; Remita, H.; Marignier, J. L.; Delcourt, M. O. *New J. Chem.* **1998**, 1239.

(9) Treguer, M.; de Cointet, C.; Remita, S.; Khatouri, M.; Mostafavi, M.; Amblard, J.; Belloni, J. *J. Phys. Chem. B* **1998**, *102*, 4310.

(10) Marignier, J. L.; Belloni, J.; Delcourt, M. O.; Chevalier, J. P. *Nature* **1985**, *317*, 344.

(11) Remita, H.; Khatouri, M.; Treguer, M.; Amblard, J.; Belloni, J. *Z. Phys. D* **1997**, *40*, 127.

(12) Remita, H.; Mostafavi, M.; Delcourt, M. O. *Radiat. Phys. Chem.* **1996**, *47*, 275.

(13) Doudna, C. M.; Hund, J. H.; Bertino, M. F. *Int. J. Mod. Phys.* B **2001**, *15*, 3302.

(14) Doudna, C. M.; Bertino, M. F.; Tokuhiro, A. T. *Langmuir* **2002**, *18*, 2434.

(15) Henglein, A. *Isr. J. Chem.* **1993**, *33*, 77.

(16) University of Missouri − Rolla's reactor is a pool reactor with a maximum power of 200 kW that employs ^{235}U fuel rods.

(17) Schatz, T.; Cook, A. R.; Meisel, D. *J. Phys. Chem. B* **1998**, *102*, 7225, and *J. Phys. Chem. B* **1999**, *103*, 10209.

(18) Zacheis, G. A.; Gray, K. A.; Kamat, P. V. *J. Phys. Chem. B* **1999**, *103*, 2142.

(19) Kreibig, U.; Gartz, M.; Hilger, A. *Ber. Bunsen-Ges. Phys. Chem.* **1997**, *101*, 1593.

(20) Liz-Marzan, L. M.; Giersig, M.; Mulvaney, P. *Langmuir* **1996**, *12*, 4329.

(21) Martino, A.; Sault, A. G.; Kawola, J. S.; Boespflug, E.; Phillips, M. L. F. *J. Catal.* **1999**, *187*, 30.

(22) Leventis, N.; Elder, I. A.; Long, G. J.; Rolison, D. R. *Nano Lett.* **2002**, *2*, 63.

(23) Huang, Z.-Y.; Mills, G.; Hajek, B. *J. Phys. Chem.* **1993**, *97*, 11542.

(24) Moulder, J. F.; Stickle, W. F.; Sobol, P. E.; Bomben, K. D. *Handbook of X-ray Photoelectron Spectroscopy*; Chastain, J., Ed.; Perkin-Elmer: Eden Prairie, MN, 1992.